Chemical Papers (2023) 77:3641–3649
https://doi.org/10.1007/s11696-023-02726-2

ORIGINAL PAPER

Microwave-assisted synthesis of N-doped carbon quantum dots for detection of methyl orange in saffron

Tahir ul Gani Mir[1] · Saurabh Shukla[1] · Azad Qayoom Malik[2] · Jaskaran Singh[3] · Deepak Kumar[2]

Received: 8 September 2022 / Accepted: 11 February 2023 / Published online: 27 February 2023

Abstract
In this study, a simple one-step microwave synthesis of nitrogen-doped carbon quantum dots (NCQDs) was performed using succinic acid as a carbon and gallic acid as a nitrogen source. Different techniques such as fluorescence spectroscopy, transmission electron microscopy, X-ray photoelectron spectroscopy (XPS), X-ray diffraction (XRD), and zeta potential analyzer were used for the characterization of as-synthesized NCQDs. The chemical composition and morphological features are analyzed by XRD and XPS spectroscopy. According to TEM investigations, these QDs exhibit a narrow size distribution ranging from 2 to 10, with maximum distribution at 6 nm. The maximum fluorescence intensity (FL intensity) of NCQDs was obtained at an excitation wavelength of 340 nm. The synthesized NCQDs were used as an effective fluorescent probe for the detection of MO with a detection limit of 0.77 µM. Moreover, the synthesized NCQDs gave satisfactory results when used for the detection of MO in saffron samples, with a recovery range of 98.6–99.2%. This study confirms that N-doped carbon quantum dots can be used as a potential candidate for the detection of MO in saffron.

Keywords Carbon quantum dots · Methyl orange · Saffron · Fluorescent detection

Introduction

Carbon-based materials, such as graphene, carbon nanotubes, fullerene, and carbon quantum dots (CQDs), have sparked significant interest among the global scientific community because of their optoelectronic applications (Ying Lim et al. 2015; Reshma and Mohanan 2019; ul Gani Mir 2022). Fluorescent CQDs with sizes ranging from 1 to 10 nm and functional group-rich surfaces have been extensively used in sensing environmental and food contaminants (Xiong et al. 2022; Manikandan and Lee 2022; Malik and Mir 2023). These CQDs exhibit attractive biocompatibility, photostability, and excitation dependents' fluorescence emission (Atchudan and Edison 2021). CQDs are superior to organic dyes and conventional semiconductor quantum dots in terms of biocompatibility, solubility, toxicity, and photostability (Resch-Genger et al. 2008). Several techniques have been established for synthesizing CQDs with desirable potential applications in sensing (Sapsford et al. 2006), bioimaging (Kairdolf et al. 2013), drug delivery (Probst et al. 2013), optoelectronic devices, etc. (Wu et al. 2015). Because of their remarkable properties and broad uses, various efficient techniques for synthesizing fluorescent CQDs have been established. These methods have been classified as top-down and bottom-up (Singh et al. 2018; Oliveira and Silva Abreu 2021; Baig et al. 2021; Cui et al. 2021). Physical or chemical cutting treatments, such as arc discharge, electrochemical oxidation, chemical oxidation, and laser ablation, are examples of top-down approaches for synthesizing CQDs. Bottom-up approaches for fabricating fluorescent CQDs, on the other hand, are gaining high popularity. Microwave irradiation, hydrothermal treatment, thermal breakdown, and plasma treatment are some approaches for synthesizing fluorescent CQDs by using ordinary organic compounds as carbon precursors (Khayal et al. 2021). The fluorescence of CQDs is highly sensitive to

✉ Tahir ul Gani Mir
mirtahirulgani@gmail.com

✉ Saurabh Shukla
sau47bt@gmail.com

1 School of Bioengineering and Biosciences, Lovely Professional University, Phagwara, Punjab 144411, India

2 School of Chemical Engineering and Physical Sciences, Lovely Professional University, Phagwara, Punjab 144411, India

3 Department of Forensic Science, Geeta University, Naultha, Panipat 132145, India

external conditions like pH, temperature, and the composition of the solvent media. In terms of pH and temperature, it has been found that in some cases, the FL intensity of CQDs is highest in neutral conditions; however, in some cases, an increase in FL intensity has been observed by varying from acidic to basic conditions. An increase in temperature may also increase the FL intensity of CQDs or vice versa (Huo et al. 2021; Wang et al. 2019; Yoo et al. 2019; Wang and Hu 2014).

Saffron is considered one of the most expensive spices in the world. It is obtained from the dried stigmas of *Crocus sativus* flowers (Mir et al. 2022). Because of its high demand, low production and extensive labor work make saffron highly expensive. The therapeutic application of saffron and its phytochemicals against several diseases makes its demand high in pharmacological industries (Mir et al. 2022; Wani et al. 2023; Mir et al. 2022). To regulate demand and save manufacturing costs, several adulterants such as safflower, flower petals, and grassroots and organic dyes are added with saffron (Kumari et al. 2021; Mir et al. 2022). Methyl orange [(MO) dimethylaminoazobenzenesulfonate] is the most prevalent artificial color used as an adulterant in saffron (Ashok et al. 2017). It is mostly used in powdered saffron and imparts orange color to the stigmas of various flowers used as adulterants in saffron. MO is also employed in various foodstuffs where saffron is used as a coloring ingredient. When dissolved in water, it displays a vivid orange hue and has a high colorability. MO contains aromatic and –N=N– groups (Fig. 1), which are extremely poisonous, teratogenic, and carcinogenic (Haque et al. 2021; Wu et al. 2021). In order to regulate the sale of unhealthy saffron or adulterated saffron and to ensure food quality and safety, the development of an inexpensive, environmental-friendly, quick, and dependable technique for the detection of MO in adulterated saffron and other foodstuffs has been the center of interest for several researchers across the globe. Several techniques have been developed to detect the presence of several organic dyes in saffron. High-performance Liquid Chromatography (HPLC), Nuclear Magnetic Raman Spectroscopy (NMR), Capillary Electrophoresis, and so on have widely been used in the detection of dyes in saffron and other foodstuffs (Kumari et al. 2021). Although these approaches were quantitative, they were time-consuming, required enormous sample volumes, produced a lot of waste, and required bulky and costly gear. As a result, a simple, quick, and sensitive approach for detecting dyes in foodstuffs is widely desired.

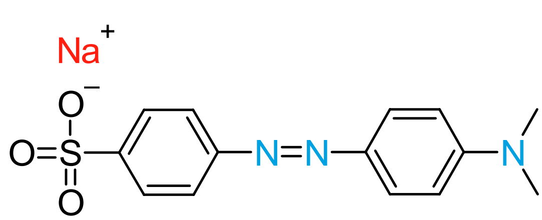

Fig. 1 Chemical structure of methyl orange

The addition of illegal and banned additives such as MO, Sudan I, melamine, and tetrazine in a foodstuff has posed a threat to human health (Thangaraju et al. 2021; Visciano and Schirone 2021; Guo et al. 2021). CDs have been employed for sensing various pollutants such as Rhodamine 6 G (Rh6G) (Bogireddy et al. 2020), Methylene Blue (MB) (Atchudan et al. 2020), Bromophenol blue (BrPB) (Shanker Sahu et al. 2021), and methyl orange (MO) (Atchudan et al. 2020). Xu et al. revealed the eco-friendly method of synthesizing CQDs by hydrothermal process and employed it as a fluorescence probe for selective and sensitive tartrazine detection in steamed bread, candy, and honey (Xu et al. 2015). Yang et al. synthesized N, Cl-doped fluorescent CQDs with a QY of 60.52%, which were used to detect tartrazine in beverages (Yang et al. 2020). CQDs with molecularly imprinted polymer (MIP) have also been used to detect tetrazine in saffron (Zoughi et al. 2021). Su et al. synthesize CQDs using cigarette filters as a carbon source for detecting Sudan I in chili and tomato samples (Anmei et al. 2018). Au@CQDs have been employed for the detection of melamine in milk with a LOD of 3.6 $nmol^{-1}$ (Hu et al. 2019). MO is one of the theses food additives that has been banned because of its negative health consequences. Several methods have also been formulated for detecting methyl orange in real samples. Zulfajri et al. (2019) used a hydrothermal process for the synthesis of CQDs from fruit extract of *Averrhoa carambola* (Zulfajri et al. 2019). These synthesized CQDs from *A. carambola* were successfully used to detect MO in water samples.

Several studies have been conducted to dope CQDs with other elements in order to increase their FL intensity and specificity for target elements (Sobiech et al. 2021; Chiu et al. 2016; Manzoor et al. 2009; Nsibande and Forbes 2016). Here, within this study, we proposed a one-step microwave-assisted synthesis of nitrogen-doped CQDs (NCQDs) for fluorescent detection of MO in adulterated saffron samples. So far, to our knowledge, there have been only instrumental-based studies (HPLC, NMR, GC–MS, etc.) for the quantification and detection of MO in saffron. Our proposed method proved significantly more selective and specific, with a low limit of detection (LOD) for the quantification and detection of MO in saffron samples.

Experimental details

Chemicals and instruments

All the chemicals used in this study were of analytical grade. Succinic acid and gallic acid were obtained from Sigma Aldrich. L-serine, L-tryptophan, L-threonine, vitamin B_6, vitamin B_1, vitamin C, CuCl2, $MgSO_4$, $NiSO_4$, NaCl, KCl, NaOH, and HCL were purchased from Loba Chemie. Phosphate citrate buffer was obtained from SRL Chemical. Ultrapure DI water was used in all the experiments.

The morphology NCQDs was confirmed by transmission electron microscopy (TEM). The surface charge and average diameter of NCQDs were determined by zeta potential and particle analyzer *(Malvern)*. Fluorescence (FL) spectroscopy was performed on a Perkin Elmer fluorescence spectrophotometer using a 5/5-nm slit. Fourier transform infrared (FTIR) spectra of NCQDs in the range of 400–4000 cm^{-1} was recorded using an FTIR spectrophotometer *(SHIMADZU AIM-8800)*. X-ray diffraction *(BRUKER D8 ADVANCE)* was used to investigate the crystalline structure of the compound. The absorption spectra were recorded using a UV–Vis double-beam spectrophotometer *(UV-1900I-SHIMADZU)*. XPS analysis was carried out to determine the elemental composition of NCQDs.

Preparation of NCQDs

The microwave-assisted approach was used for the quick synthesis NCQDs using succinic acid as a carbon and gallic acid as a nitrogen source. Briefly, an optimized amount of 1 g of succinic acid and 0.7 g of gallic acid were mixed in deionized water (5 mL). Next, a 700-W home microwave oven was used to heat the solution for 10 min resulting in the formation of brown material. The mixture was then cooled at room temperature and then dissolved in 10 ml of water. The solution was then centrifuged at 10,000 rpm for 20 min to eliminate unreactive and large particles. The resulting supernatant was then filtered and then stored for characterization and future use.

Optimization of prepared NCQDs

The effect of pH values (4–10) on NCQDs was investigated in order to determine their fluorescent behavior for different pf values. The pH of NCQDs was adjusted using 0.1 mM HCL and NaOH solutions. The optimized time needed for effective quenching of the FL intensity of NCQDs upon interaction with MO was also monitored at different time intervals.

Preparation of the fluorescent probe for MO using NCQDs

For selective interaction of NCQDs with MO, 100 µL MO solutions with different concentrations (02–200 µM) were added into an Eppendorf tube containing 800 µL of NCQDs (pH 8 with phosphate buffer). The fluorescence spectra were obtained at an excitation wavelength of 340 nm after 3 min of incubation time.

Collection and preparation of saffron samples

Saffron samples were collected from local markets of Pampore, Kashmir, India. The Pampore district of Kashmir is known for its quality cultivation of saffron. The collected saffron samples were analyzed using the ISO-3632 method to ensure that samples were free from adulteration. The sample was grounded into powder form using a mortar and pestle. About 100 mg of grounded sample was then taken into a screw-caped test tube, and 100 ml of water was added. The mixture was sonicated for 30 min and centrifuged for about 30 min at 10,000 rpm. The resulting supernatant was filtered and stored at 4 °C for further use.

Detection of MO in saffron samples using NCQDs

The detection of MO in saffron was performed by spiking different concentrations of MO (5–75 µL) to saffron extract (100 µL), and NCQDs were added to the final concentration of 500 µL. The fluorescence spectra of samples were taken, and the recovery percentage was calculated using the following relation:

$$R = \left[\left(C_3 - C_2\right)/C_1\right] \times 100\%, \tag{1}$$

where R recovery percentage, C_1 added concentration of MO, C_2 real MO concentration already present in the sample, and C_3 concentration of MO found after adding standard MO.

Results

Characterization of NCQDs

The fluorescence emission characteristics of NCQDs are wavelength dependent. Excitation-dependent fluorescence spectra are produced by the surface-state emissive trap when different excitation wavelengths are used. As the excitation wavelength increases from 280 to 440 nm, the emission peaks move from 355 to 498 nm (Fig. 2). Furthermore, at 340 nm of excitation, the emission intensity reached maximum.

The FTIR spectra of NCQDs exhibit distinctive absorption peaks at 1636, 2945, and 3340 cm^{-1}. These peaks correspond to C=O, C–H, and O–H stretching vibrations, respectively (Fig. 3a). The narrow peak observed at 1404 cm^{-1} is due to the presence of O–H in-plane deformation. Similarly, the presence of the C–O vibration of the C–O–C peak can be seen at 1066 cm^{-1}. There are numerous distinct bands in the spectrum of NCQDs that can be

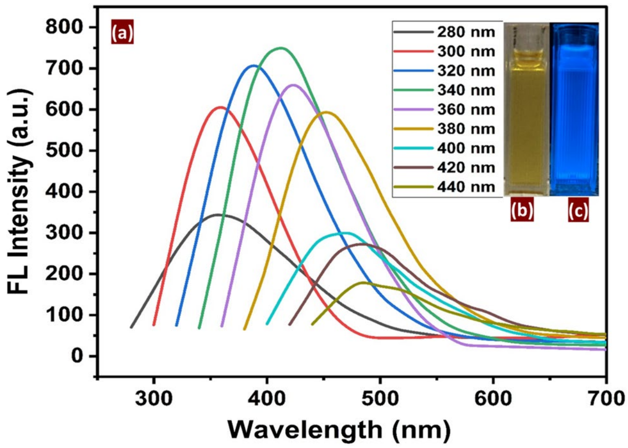

Fig. 2 Fluorescence spectra NCQDs excited from 280 to 440 nm (**a**). NCQDs under visible light (**b**) and UV light (**c**)

found between 1210 and 1636 cm^{-1}. These bands correlate to the stretching vibration that is unique to CN bonds.

In order to perform XRD analysis, the as-prepared NCQDs were drop-coated onto a glass sheet (1 × 1 cm^2), and the analysis was performed. Figure 3b depicts typical XRD patterns for as-prepared NCQDs. In the XRD patterns, a wide peak centered at around 21.02^0 could be found, which is almost similar to the graphite lattice spacing (20.73°). This lattice contraction in the above-mentioned range is typical for nanomaterials in the nanoscale domain, and it is most likely owing to the microwave process creating abundant active sites on the surface of NCQDs. Furthermore, XRD results confirm the 3.5 A lattice spacing.

Electrophoretic light scattering was used to determine the zeta potential of the dispersed NCQDs. Electrophoretic light scattering revealed that the zeta potentials of NCQDs were—3.4 mV (Fig. 4a). Each sample was subjected to comparable zeta potential and particle size distribution measurements. The zeta potential represents not only the electrical charge on the particle surface but also the stability of colloidal dispersions. The average particle size of NCQDs was found to be approximately 6 nm (Fig. 4b). The results of the particle size distributions agree with the zeta potential measurement.

TEM observations were used to determine the size and morphology of the prepared NCQDs. Figure 4c demonstrates that the samples are made up of a large number of spherical nano-dots with an average diameter of 6 nm. The enlarged TEM images in Fig. 4c show that the quantum dots' average lateral dimension is less than 10 nm. As illustrated in Fig. 4d, the statistical size distribution of NCQDs shows that the size falls within the range of 3–10 nm with maximum distribution at 6 nm.

X-ray photoelectron spectroscopy was used to investigate the chemical composition and structure of the N-CDs (XPS). Figure 5a depicts a general overview of the N-CD XPS spectrum. O1s, N1s, and C1s were assigned strong binding energy peaks at 284.53, 531.24, and 399.34 eV, respectively. The N-CDs were made up of C (62.05%), N (15.88%), and O (22.07%). Moreover, in the high-resolution spectrum of C1s, two peaks at 283.14 and 287.81 eV were attributed to C–C and C=N/C=O bonds, respectively, as shown in Fig. 5b. The two notable peaks at 399.55 and 401.1 eV in the N1s spectrum were assigned to N–(C)$_3$ and O=N–C, respectively (Fig. 5c). The two central peaks in the O1s spectrum (Fig. 5d) at 530.29 and 532.54 were attributed to C–O and C=O/N=O, respectively. The XPS spectrum showed that the N-CDs were composed of three different elements: carbon, nitrogen, and oxygen. Additionally, the surface of the N-CDs had several oxygen-containing groups as well as nitrogen groups.

Effect of MO on the FL intensity of NCQDs

The FL intensity of NCQDs under the influence of different concentrations of MO (02–200 µM) was studied. It is evident from Fig. 6 that the FL intensity of NCQDs decreases with an increase in the concentration of MO. The fluorescence quenching of NCQDs with different concentrations of MO is due to charge transfer or energy transfer between the fluorophore and the quencher. Charge transfer occurs between the quencher and the excited molecule of the fluorophore.

Fig. 3 FTIR (**a**) and XRD (**b**) of NCQDs

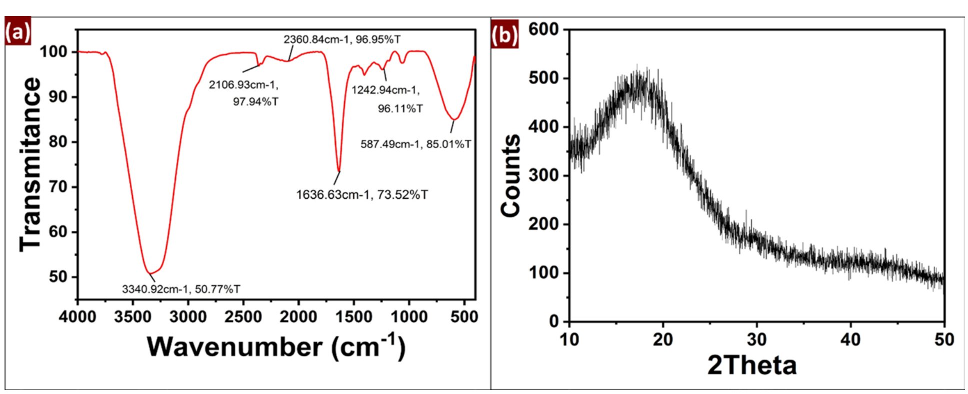

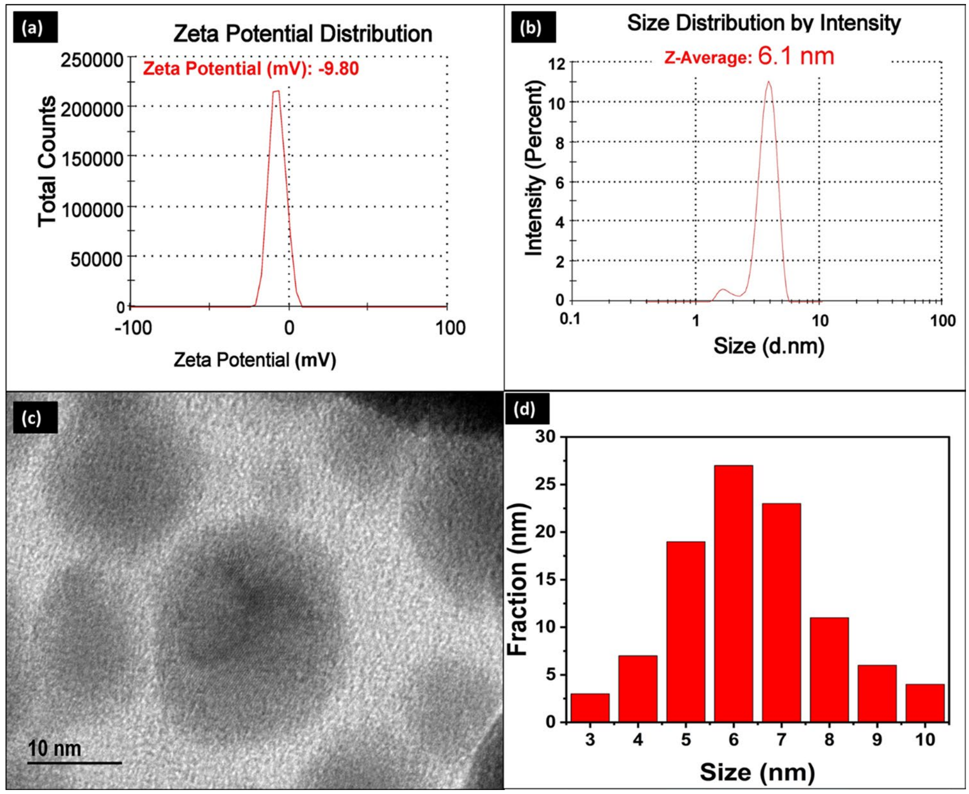

Fig. 4 Zeta potential distribution (**a**), size distribution (**b**), TEM (**c**), and size distribution, (**d**) of NCQDs

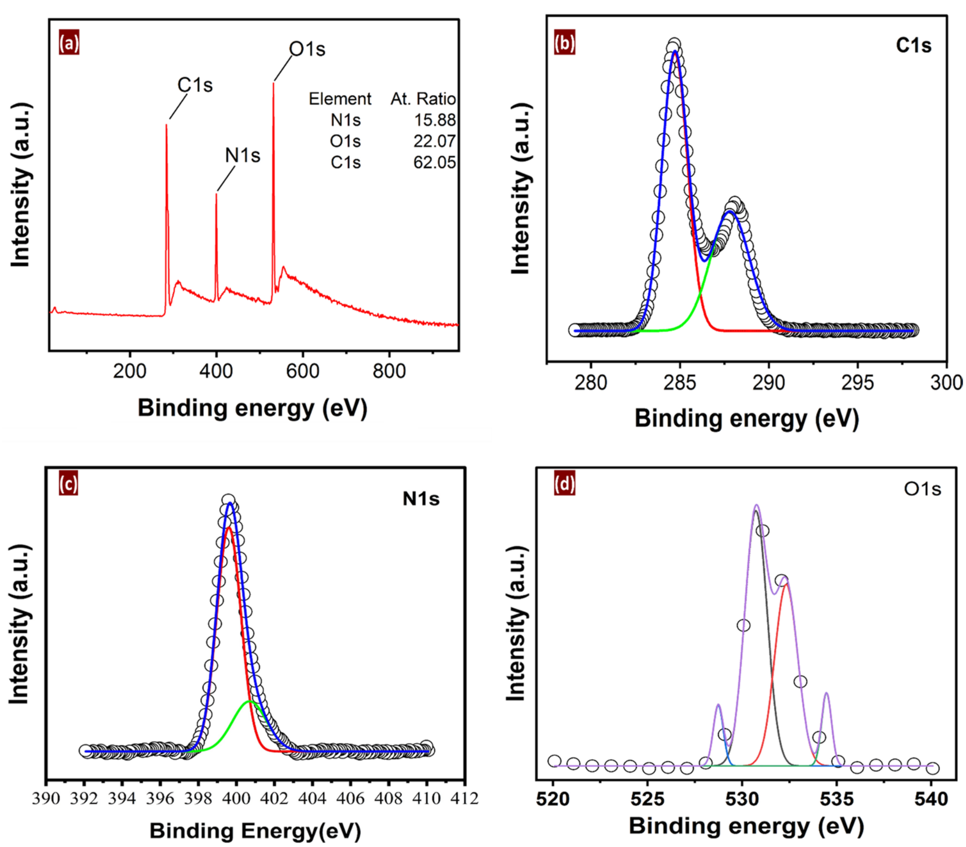

Fig. 5 XPS full scan of NCQDs (**a**), high-resolution XPS spectrum of C 1 s (**b**), N 1 s (**c**), and O 1 s (**d**)

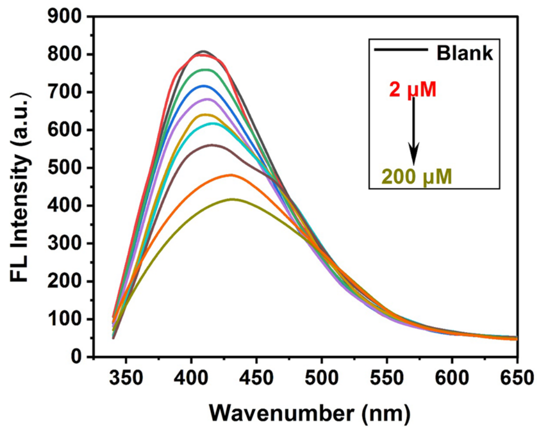

Fig. 6 Fluorescence spectra of NCQDs in the presence of different concentrations of MO (2–200 μM)

Energy transfer can occur if the fluorophore's fluorescence emission spectra and the quencher's UV absorbance spectra significantly overlap or the distance between the two is very small, often less than 10 nm. In this study, the fluorescence maxima of NCQDs can be seen at 425 nm after an excitation wavelength of 340 nm, and the maximum absorption wavelength of MO can be seen at 475 nm. It can be seen that the spectra of the two are effectively overlapped, as shown in Fig. 7a. Therefore, it is evident to say that the fluorescence quenching of MO on NCQDs is due to energy transfer between them.

Optimization

Given the observed fluorescence quenching of NCQDs in the presence of MO, the possibility of establishing a sensitive approach for MO determination was studied. The effect of pH in the range of 4–10 on the FL intensity of NCQDs was investigated. It was found that pH impacts the FL intensity of the NCQDs solution. While the relative FL intensity values (F_0/F) essentially remained constant throughout the entire pH range, the emission of NCQDs solution increased with the increase in pH from 4 to 8 and then decreased from 8 to 10 (Fig. 7b). Therefore, pH 8 was selected as the ideal solution pH for further studies. The effects of several buffer systems, including phosphate buffer, Britton–Robinson (B–R), and Tris-HCl on the F_0/F, were then investigated at pH 8. According to the findings, the phosphate buffer was the most effective buffer. Additionally, the impact of incubation time on the value of FL intensity was investigated. At normal conditions, the incubation time was optimized by measuring the FL intensity of NCQDs and MO solution (pH 8) every 5 min. The maximum FL intensity value was attained after 15 min and remained almost steady for 60 min, as shown in Fig. 7c. As a result, the ideal incubation time for FL intensity was tested 10 min later.

Fig. 7 Overlap between a fluorescence spectrum of NCQDs and absorption spectrum of MO (**a**), the effect of pH on the fluorescent intensity of NCQDS (**b**), fluorescent responses of NCQDs in the presence of MO at different intervals of time (**c**), and selectivity of NCQDS toward MO in the presence of interfering substances (**d**)

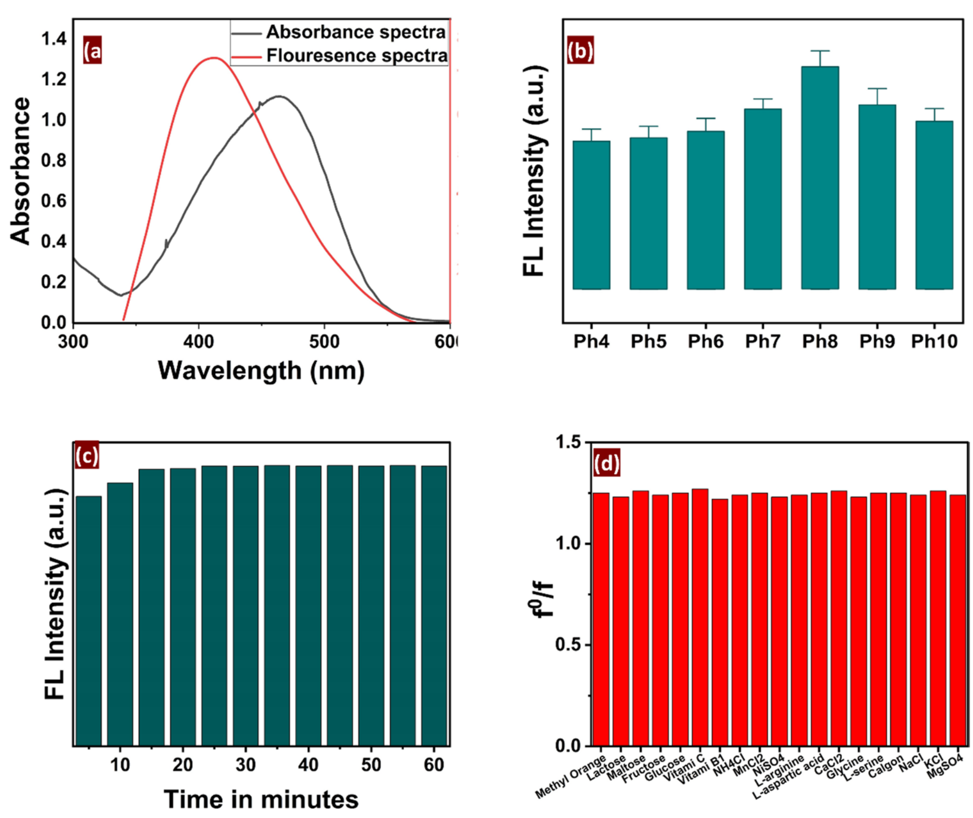

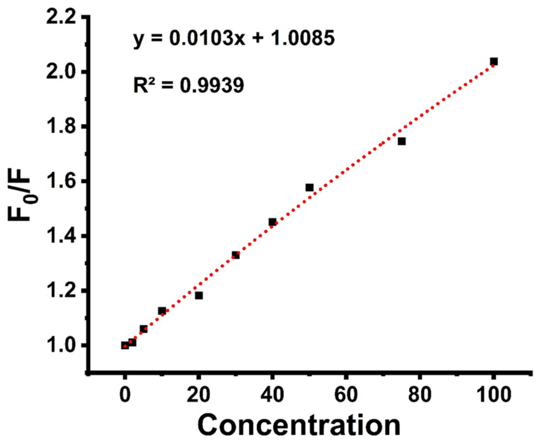

Fig. 8 Relationship between fluorescence quenching and MO at various concentrations

To assess the specificity, the effects of some potential interfering substances L-tryptophan, L-serine, L-threonine, vitamin C, vitamin B_6, vitamin B_1, $CuCl_2$, $MgSO_4$, $NiSO_4$, NaCl, and KCl were examined. Results were obtained by combining 20.0 mmol/L of MO with NCQDs alone and 22.0 mmol/L of MO and 2000 mmol/L of possible interfering chemicals with the NCQDs, respectively. As shown in Fig. 7d, there was very small to no impact on the ability of MO to quench fluorescence. As a result, the technique demonstrated high selectivity for MO detection.

Linear equation and detection limit

Figure 8 depicts the calibration curve for the detection of MO. The FL intensity of NCQDs was found to be best described by using the Stern–Volmer equation, which goes as follows: $F_0/F = K_{sv}\,[Q] + 1$, where F_0 and F are the fluorescence intensities of NCQDs in the presence and absence of MO, respectively; K_{sv} is a quenching constant, and $[Q]$ is the concentration of quencher. The MO concentration, C, was represented by the linear regression equation $F_0/F = 0.0103\text{C} + 1.0085$, where C represented mmol/L. The linear range had an R_2 of 0.993 and covered the range of 2.00–200.00 µM/L. Based on 3 s/k, the limit of detection (LOD) was 0.77 µM /L. For 22.0 mmol/L MO, the relative standard deviation (RSD) for about five replicate results was 1.3%, indicating sensitive techniques for detecting MO. A systematic to illustrate the synthesis of NCQDs and their mechanism for detection of MO is depicted in Fig. 9.

Detection of MO in saffron samples

The application of NCQDs for the detection of MO in saffron samples was investigated according to the procedures described in Sect. "Detection of MO in saffron samples using NCQDs". Briefly, 100 µL of pretreated samples of saffron spiked with different concentrations of MO, and their fluorescent detection was carried out according to the procedure mentioned in Sect. "Detection of MO in saffron samples using NCQDs". The results showed a recovery range of 97.6–98.2%, as shown in Table 1. Therefore, it is evident to say that the microwave-synthesized NCQDs can be used as an ideal candidate for the detection of MO in saffron samples. A diagrammatic representation of synthesis and application of NCQDs for detection of MO is represented in Fig. 9.

Conclusion

Saffron is one of the most expensive spices in the world. Due to its high price, low production, and high demand, this spice is highly prone to adulteration. Methyl orange is one of the most common artificial colorants used in the adulteration of saffron. To prevent the sale of adulterated saffron and to make sure that food is safe and of good quality, researchers all over the world have been attempting to come up with a cheap, quick, reliable, and environmental-friendly method for determining toxic substances in foodstuff. In this study, the NCQDs were synthesized by employing the microwave synthesis method using succinic acid and gallic acid as carbon and nitrogen sources, respectively. The characterization of NCQDs was done by using different instrumentation techniques such as fluorescence spectroscopy, XRD, FTIR, TEM, XPS, and zeta potential. The synthesized NCQDs were used as an effective fluorescent probe for the detection of MO with a detection limit of 0.77 µM. Moreover, the as-synthesized NCQDs showed remarkable results when used

Table 1 Quantitative measurement of spiked MO in saffron tea using NCQDS

Sample	MO found (µM/L)	MO added (µM/L)	Final found value (µM/L)	Recovery (%)	RSD (%)
Saffron	0.00	10.00	9.82 ± 0.04	99.2	1.8
	0.00	25.00	24.50	99.0	1.2
	0.00	50.00	48.80 ± 0.05	98.6	1.4
	0.00	75.00	73.00	98.33	1.6
	0.00	100.00	97.90 ± 0.03	98.9	1.7

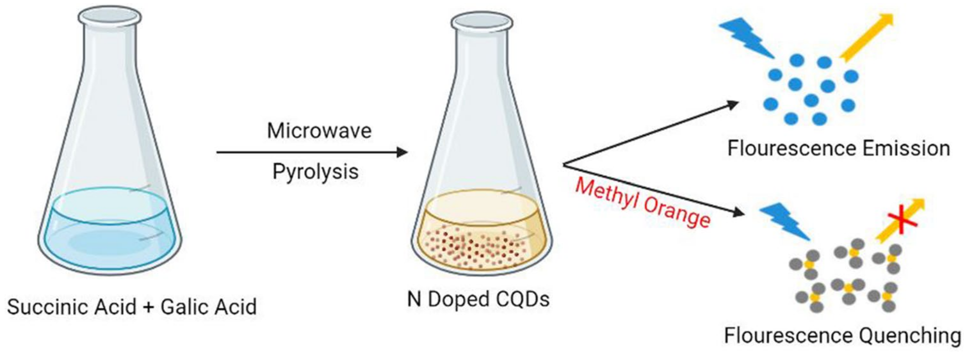

Fig. 9 Scheme for synthesis of NCQDs and their application in detection of MO

to detect MO in samples of saffron, with a recovery range of 98.6–99.2%. Therefore, this study confirms that N-doped carbon quantum dots could be used to find MO in saffron.

Funding None.

Declarations

Conflict of interest The authors declare that they have no conflict of interest.

Ethical approval Not applicable.

References

Anmei S, Qingmei Z, Yuye C, Yilin W (2018) Preparation of carbon quantum dots from cigarette filters and its application for fluorescence detection of Sudan I. Anal Chim Acta 1023:115–120. https://doi.org/10.1016/j.aca.2018.03.024

Ashok V, Agrawal N, Esteve-Romero J, Bose D, Dubey NP (2017) Detection of methyl orange in saffron and other edibles using direct injection micellar liquid chromatography. Food Anal Methods 10:269–276. https://doi.org/10.1007/s12161-016-0578-3

Atchudan R, Edison TNJI, Mani S, Perumal S, Vinodh R, Thirunavukkarasu S, Lee YR (2020) Facile synthesis of a novel nitrogen-doped carbon dot adorned zinc oxide composite for photodegradation of methylene blue. Dalton Trans 49:17725–17736. https://doi.org/10.1039/D0DT02756A

Atchudan R, Edison TNJI, Shanmugam M, Perumal S, Somanathan T, Lee YR (2021) Sustainable synthesis of carbon quantum dots from banana peel waste using hydrothermal process for in vivo bioimaging. Phys E Low-Dimens Syst Nanostruct 126:114417. https://doi.org/10.1016/j.physe.2020.114417

Baig N, Kammakakam I, Falath W (2021) Nanomaterials: a review of synthesis methods, properties, recent progress, and challenges. Mater Adv 2:1821–1871. https://doi.org/10.1039/D0MA00807A

Bogireddy NKR, Lara J, Fragoso LR, Agarwal V (2020) One-step hydrothermal preparation of highly stable N doped oxidized carbon dots for toxic organic pollutants sensing and bioimaging. Chem Eng J 401:126097. https://doi.org/10.1016/j.cej.2020.126097

Chiu S-H, Gedda G, Girma WM, Chen J-K, Ling Y-C, Ghule AV, Ou K-L, Chang J-Y (2016) Rapid fabrication of carbon quantum dots as multifunctional nanovehicles for dual-modal targeted imaging and chemotherapy. Acta Biomater 46:151–164. https://doi.org/10.1016/j.actbio.2016.09.027

Cui L, Ren X, Sun M, Liu H, Xia L (2021) Carbon Dots: Synthesis. Prop Appl Nanomater 11:3419. https://doi.org/10.3390/nano11123419

de Oliveira BP, da Silva Abreu FOM (2021) Carbon quantum dots synthesis from waste and by-products: perspectives and challenges. Mater Lett 282:128764. https://doi.org/10.1016/j.matlet.2020.128764

Guo Y, Girmatsion M, Li H-W, Xie Y, Yao W, Qian H, Abraha B, Mahmud A (2021) Rapid and ultrasensitive detection of food contaminants using surface-enhanced Raman spectroscopy-based methods. Crit Rev Food Sci Nutr 61:3555–3568. https://doi.org/10.1080/10408398.2020.1803197

Haque MdM, Haque MdA, Mosharaf MK, Marcus PK (2021) Decolorization, degradation and detoxification of carcinogenic sulfonated azo dye methyl orange by newly developed biofilm consortia, Saudi. J Biol Sci 28:793–804. https://doi.org/10.1016/j.sjbs.2020.11.012

Hu X, Shi J, Shi Y, Zou X, Arslan M, Zhang W, Huang X, Li Z, Xu Y (2019) Use of a smartphone for visual detection of melamine in milk based on Au@Carbon quantum dots nanocomposites. Food Chem 272:58–65. https://doi.org/10.1016/j.foodchem.2018.08.021

Huo X, Shen H, Liu R, Shao J (2021) Solvent effects on fluorescence properties of carbon dots: implications for multicolor imaging. ACS Omega 6:26499–26508. https://doi.org/10.1021/acsomega.1c03731

Kairdolf BA, Smith AM, Stokes TH, Wang MD, Young AN, Nie S (2013) Semiconductor quantum dots for bioimaging and biodiagnostic applications. Annu Rev Anal Chem Palo Alto Calif 6:143–162. https://doi.org/10.1146/annurev-anchem-060908-155136

Khayal A, Dawane V, Amin MA, Tirth V, Yadav VK, Algahtani A, Khan SH, Islam S, Yadav KK, Jeon B-H (2021) Advances in the methods for the synthesis of carbon dots and their emerging applications. Polymers 13:3190. https://doi.org/10.3390/polym13183190

Kumari L, Jaiswal P, Tripathy SS (2021) Various techniques useful for determination of adulterants in valuable saffron: a review. Trends Food Sci Technol 111:301–321. https://doi.org/10.1016/j.tifs.2021.02.061

Malik AQ, T. ul G. Mir, D. Kumar, (2023) An overview of paclitaxel and molecular imprinted polymers capped with quantum dots as an alternative approach for paclitaxel extraction and detection. Curr Mater Sci 16:185–216

Manikandan V, Lee NY (2022) Green synthesis of carbon quantum dots and their environmental applications. Environ Res 212:113283. https://doi.org/10.1016/j.envres.2022.113283

Manzoor K, Johny S, Thomas D, Setua S, Menon D, Nair S (2009) Bio-conjugated luminescent quantum dots of doped ZnS: a cyto-friendly system for targeted cancer imaging. Nanotechnology 20:065102. https://doi.org/10.1088/0957-4484/20/6/065102

Nsibande SA, Forbes PBC (2016) Fluorescence detection of pesticides using quantum dot materials–a review. Anal Chim Acta 945:9–22. https://doi.org/10.1016/j.aca.2016.10.002

Probst CE, Zrazhevskiy P, Bagalkot V, Gao X (2013) Quantum dots as a platform for nanoparticle drug delivery vehicle design. Adv Drug Deliv Rev 65:703–718. https://doi.org/10.1016/j.addr.2012.09.036

Resch-Genger U, Grabolle M, Cavaliere-Jaricot S, Nitschke R, Nann T (2008) Quantum dots versus organic dyes as fluorescent labels. Nat Methods 5:763–775. https://doi.org/10.1038/nmeth.1248

Reshma VG, Mohanan PV (2019) Quantum dots: applications and safety consequences. J Lumin 205:287–298. https://doi.org/10.1016/j.jlumin.2018.09.015

Sapsford KE, Pons T, Medintz IL, Mattoussi H (2006) Biosensing with luminescent semiconductor quantum dots. Sensors 6:925–953. https://doi.org/10.3390/s6080925

Shanker Sahu R, Dubey A, Shih Y (2021) Novel metal-free in-plane functionalized graphitic carbon nitride with graphene quantum dots for effective photodegradation of 4-bromophenol. Carbon 182:89–99. https://doi.org/10.1016/j.carbon.2021.05.033

Singh I, Arora R, Dhiman H, Pahwa R (2018) Carbon quantum dots: synthesis, characterization and biomedical applications. Turk J Pharm Sci 15:219–230. https://doi.org/10.4274/tjps.63497

Sobiech M, Luliński P, Wieczorek PP, Marć M (2021) Quantum and carbon dots conjugated molecularly imprinted polymers as advanced nanomaterials for selective recognition of analytes in environmental, food and biomedical applications. TrAC Trends Anal Chem 142:116306. https://doi.org/10.1016/j.trac.2021.116306

Thangaraju S, Modupalli N, Natarajan V (2021) Food adulteration and its impacts on our health/balanced nutrition. In: Food Chem, John Wiley and Sons, Ltd pp 189–216 https://doi.org/10.1002/9781119792130.ch7.

TUG Mir, A Khurshid Wani, J Singh (2022) Crocus sativus: comprehensive pharmacological significance and forensic identification of saffron in illegal trade https://doi.org/10.21088/ijfmp.0974.3383.14221.38.

ulGani Mir T, Malik AQ, Singh J, Shukla S, Kumar D (2022) An overview of molecularly imprinted polymers embedded with quantum dots and their implementation as an alternative approach for extraction and detection of crocin. ChemistrySelect 7:e202200829. https://doi.org/10.1002/slct.202200829

ulMir TG, Singh J, Shukla S (2022) Quantification of apocarotenoids in commercial Indian (Kashmiri) saffron using UV-Vis spectroscopy and HPLC analysis. Acta Agric Slov. 118:1–9. https://doi.org/10.14720/aas.2022.118.3.2333

ulMir TG, Wani AK, Singh J, Shukla S (2022) Therapeutic application and toxicity associated with crocus sativus (saffron) and its phytochemicals. Pharmacol Res Mod Chin Med 4:100136. https://doi.org/10.1016/j.prmcm.2022.100136

Visciano P, Schirone M (2021) Food frauds: global incidents and misleading situations. Trends Food Sci Technol 114:424–442. https://doi.org/10.1016/j.tifs.2021.06.010

Wang Y, Hu A (2014) Carbon quantum dots: synthesis, properties and applications. J Mater Chem c 2:6921–6939. https://doi.org/10.1039/C4TC00988F

Wang X, Feng Y, Dong P, Huang J (2019) A mini review on carbon quantum dots: preparation, properties, and electrocatalytic application. Front Chem 7:671. https://doi.org/10.3389/fchem.2019.00671

Wani AK, Akhtar N, Mir TG, Singh R, Jha PK, Mallik SK, Sinha S, Tripathi SK, Jain A, Jha A, Devkota HP, Prakash A (2023) Targeting apoptotic pathway of cancer cells with phytochemicals and plant-based nanomaterials. Biomolecules 13:194. https://doi.org/10.3390/biom13020194

Wu J, Chen S, Seeds A, Liu H (2015) Quantum dot optoelectronic devices: lasers, photodetectors and solar cells. J Phys Appl Phys 48:363001. https://doi.org/10.1088/0022-3727/48/36/363001

Wu L, Liu X, Lv G, Zhu R, Tian L, Liu M, Li Y, Rao W, Liu T, Liao L (2021) Study on the adsorption properties of methyl orange by natural one-dimensional nano-mineral materials with different structures. Sci Rep 11:10640. https://doi.org/10.1038/s41598-021-90235-1

Xiong J, Zhang H, Qin L, Zhang S, Cao J, Jiang H (2022) Magnetic fluorescent quantum dots nanocomposites in food contaminants analysis: current challenges and opportunities. Int J Mol Sci 23:4088. https://doi.org/10.3390/ijms23084088

Xu H, Yang X, Li G, Zhao C, Liao X (2015) Green synthesis of fluorescent carbon dots for selective detection of tartrazine in food samples. J Agric Food Chem 63:6707–6714. https://doi.org/10.1021/acs.jafc.5b02319

Yang X, Xu J, Luo N, Tang F, Zhang M, Zhao B (2020) N, Cl co-doped fluorescent carbon dots as nanoprobe for detection of tartrazine in beverages. Food Chem 310:125832. https://doi.org/10.1016/j.foodchem.2019.125832

Ying Lim S, Shen W, Gao Z (2015) Carbon quantum dots and their applications. Chem Soc Rev 44:362–381. https://doi.org/10.1039/C4CS00269E

Yoo D, Park Y, Cheon B, Park M-H (2019) Carbon dots as an effective fluorescent sensing platform for metal ion detection. Nanoscale Res Lett 14:272. https://doi.org/10.1186/s11671-019-3088-6

Zoughi S, Faridbod F, Amiri A, Ganjali MR (2021) Detection of tartrazine in fake saffron containing products by a sensitive optical nanosensor. Food Chem 350:129197. https://doi.org/10.1016/j.foodchem.2021.129197

Zulfajri M, Dayalan S, Li W-Y, Chang C-J, Chang Y-P, Huang GG (2019) Nitrogen-doped carbon dots from averrhoa carambola fruit extract as a fluorescent probe for methyl orange. Sensors 19:5008. https://doi.org/10.3390/s19225008